The Shape of the Initial Cluster Mass Function: What It Tells Us about the Local Star Formation Efficiency — **Source link**

Genevieve Parmentier, Genevieve Parmentier, Simon P. Goodwin, Pavel Kroupa ...+1 more authors

Institutions: University of Bonn, University of Liège, University of Sheffield

Related papers:

- Embedded Clusters in Molecular Clouds

- A comprehensive set of simulations studying the influence of gas expulsion on star cluster evolution

- The effect of mass loss on the dynamical evolution of a stellar system - Analytic approximations

- The influence of residual gas expulsion on the evolution of the Galactic globular cluster system and the origin of the Population II halo

- The formation and early dynamical evolution of bound stellar systems.

THE SHAPE OF THE INITIAL CLUSTER MASS FUNCTION: WHAT IT TELLS US ABOUT THE LOCAL STAR FORMATION EFFICIENCY

G. PARMENTIER,[1,2,3] S. P. GOODWIN,[4] P. KROUPA,[1] AND H. BAUMGARDT[1]
Received 2007 December 13; accepted 2008 February 6

ABSTRACT

We explore how the expulsion of gas from star cluster forming cloud cores due to supernova explosions affects the shape of the initial cluster mass function, that is, the mass function of star clusters when effects of gas expulsion are over. We demonstrate that if the radii of cluster-forming gas cores are roughly constant over the core mass range, as supported by observations, then more massive cores undergo slower gas expulsion. Therefore, for a given star formation efficiency, more massive cores retain a larger fraction of stars after gas expulsion. The initial cluster mass function may thus differ from the core mass function substantially, with the final shape depending on the star formation efficiency. A mass-independent star formation efficiency of ∼20% turns a power-law core mass function into a bell-shaped initial cluster mass function, while mass-independent efficiencies of order 40% preserve the shape of the core mass function.

Subject headings: galaxies: star clusters — stars: formation — stellar dynamics

1. INTRODUCTION

One of the greatest discoveries made by the *Hubble Space Telescope* is that the formation of star clusters with mass and compactness comparable to those of old globular clusters is still ongoing in violent star-forming environments, such as starbursts and galaxy mergers. The young cluster mass function (CMF: the number of objects per logarithmic cluster mass interval, $dN/d \log m$) is often reported to be a power law of spectral index $\alpha = -2$ (i.e., equivalent to $dN \propto m^{-2} dm$) down to the detection limit (Fall & Zhang 2001; Bik et al. 2003; Hunter et al. 2003). Similar results are obtained for the cluster luminosity function (e.g., Miller et al. 1997; Whitmore et al. 1999). However, old globular cluster systems are found to have a CMF which is Gaussian-like with a peak mass of $\sim 10^5\ M_\odot$ (Kavelaars & Hanes 1997). These very different CMFs between young and old systems present the greatest dissimilarity between the two populations and perhaps the greatest barrier to identifying young massive clusters as analogs of young globular clusters.

Yet it is worth keeping in mind that the luminosity/mass distribution of some young star cluster systems does *not* obey a power law. Based on high-resolution Very Large Array observations, Johnson (2008) rules out a power-law cluster luminosity function for the young star clusters formed in the starburst galaxy Henize 2-10. In NGC 5253, an irregular dwarf galaxy in the Centaurus Group, Cresci et al. (2005) detect a turnover at $5 \times 10^4\ M_\odot$ in the mass function of the young massive star clusters in the central region. Last but not least, the case of the Antennae merger of galaxies NGC 4038/39 remains heavily debated. While Whitmore et al. (1999) infer from their *HST* WFPC2 imaging data a power-law cluster luminosity function with a spectral index $\alpha \simeq -2.1$, Anders et al. (2007) report the first statistically robust detection of a turnover at $M_V \simeq -8.5$ mag, corresponding to a mass of $\simeq 16 \times 10^3\ M_\odot$. The origin of that discrepancy likely resides in differences in the data reduction and the statistical analysis aimed

at rejecting bright-star contamination and disentangling completeness effects from intrinsic cluster luminosity function substructures.

These findings raise the highly interesting prospect that the shape of the CMF at young ages does vary from one galaxy to another. If it were conclusively proven that the shape of the initial cluster mass function (ICMF) is *not* universal among galaxies but, instead, depends on environmental conditions and/or on the star formation process, consequences would be far reaching since this would imply that the young CMF may help us decipher physical conditions prevailing in external galaxies.

In this contribution, we report the first results of a project investigating the evolution of the mass function of star-forming cores into that of bound gas-free star clusters that have survived expulsion of their residual star-forming gas. A similar study was carried out by Parmentier & Gilmore (2007) in which they showed that protoglobular cloud mass functions characterized by a mass scale of $\simeq 10^6\ M_\odot$ evolve into the observed globular cluster mass function. They propose that the origin of the universal Gaussian mass function of old globular clusters thus likely resides in a protoglobular cloud mass scale common among galaxies and imposed in the protogalactic era. Present-day star-forming cores, however, do not show any characteristic mass scale as their mass function is a power law down to the detection limit. Previously, Kroupa & Boily (2002) showed that a power-law embedded-cluster mass function can evolve into a mass function with a turnover near $10^5\ M_\odot$ if the physics of gas removal is taken into account. Taking advantage of the grid of *N*-body models recently compiled by Baumgardt & Kroupa (2007), we explore in greater detail how a featureless core mass function evolves into the ICMF as a result of gas removal, which we model as the supernova-driven expansion of a supershell of gas. We also explore how the ICMF responds to model parameter variations so as to understand what may make the mass function of young star clusters vary from one galaxy to another. In a companion paper (Baumgardt et al. 2008), we explore this issue from a different angle, that is, by defining an energy criterion, and we apply that alternative model to the mass function of the Milky Way old globular clusters.

2. NOTION OF INITIAL CLUSTER MASS FUNCTION

Before proceeding any further, it is worth defining the notion of the ICMF properly. Following the onset of massive star activity at an age of 0.5–5 Myr, a gas-embedded cluster expels its

[1] Argelander-Institut für Astronomie, University of Bonn, Auf dem Hügel 71, D-53121 Bonn, Germany.
[2] Institute of Astrophysics and Geophysics, University of Liège, Allée du 6 Août 17, B-4000 Liège, Belgium.
[3] Alexander von Humboldt Fellow and Research Fellow of Belgian Science Policy.
[4] Department of Physics and Astronomy, University of Sheffield, Hicks Building, Hounsfield Road, Sheffield S3 7RH, UK.

residual star-forming gas. As a result, the potential in which the stars reside changes rapidly, causing the cluster to violently relax in an attempt to reach a new equilibrium. This violent relaxation takes 10–50 Myr during which time the cluster loses stars ("infant weight loss") and may be completely destroyed ("infant mortality"; this process has been studied in detail by Hills 1980; Mathieu 1983; Elmegreen 1983; Lada et al. 1984; Elmegreen & Clemens 1985; Pinto 1987; Verschueren & David 1989; Goodwin 1997a,1997b; Kroupa et al. 2001; Geyer & Burkert 2001; Boily & Kroupa 2003a, 2003b; Goodwin & Bastian 2006; Baumgardt & Kroupa 2007). After ∼50 Myr the evolution of clusters is driven by internal two-body relaxation processes and tidal interactions with the host galaxy (see Spitzer 1987). Following Kroupa & Boily (2002) we define the ICMF as the mass function of clusters *at the end of the violent relaxation phase*, that is, when their age is ≃50 Myr.

The effect of gas expulsion depends strongly on the virial ratio of the cluster *immediately before* the gas is removed. If the stars and gas are in virial equilibrium before gas expulsion the virial ratio $Q_\star$ of the stars depends entirely on the star formation efficiency (SFE, or ϵ) such that $Q_\star = 1/(2\epsilon)$ (where we define virial equilibrium to be $Q = 1/2$; Goodwin 2008). Formally, ϵ is the *effective* SFE (eSFE; see Verschueren 1990; Goodwin & Bastian 2006), that is, a measure of how far from virial equilibrium the cluster is at the onset of gas expulsion, rather than the actual efficiency with which the gas has formed stars. We note that even quite small deviations from virial equilibrium can equate to large differences between the eSFE and the SFE. However, in this paper we make the assumption that the stars have had sufficient time to come into virial equilibrium with the gas potential (i.e., gas expulsion occurs after a few crossing times), and so the eSFE very closely matches the SFE. We discuss this assumption further in the conclusions.

In this case, the radius of the embedded cluster is the same as that of the core, and the three-dimensional velocity dispersion of the stars in the embedded cluster is dictated by the depth of the core gravitational potential, namely, $\sigma = (Gm_c/r_c)^{1/2}$, where m_c and r_c are the mass and radius of the core, respectively, and G is the gravitational constant.

A star-cluster forming "core" of mass m_c (i.e., the region of a molecular cloud that forms a cluster) with a SFE of ϵ will form a cluster of mass ϵm_c. However, gas expulsion will unbind a fraction $(1 - F_{\text{bound}})$ of the stars in that cluster such that the mass of the cluster at ∼50 Myr will be

$$m_{\text{init}} = F_{\text{bound}}\epsilon m_c. \qquad (1)$$

(Note that when $F_{\text{bound}} \sim 0$ the cluster is destroyed.)

It is important to keep in mind that, for clusters whose age does not exceed, say, 10–20 Myr, the mass fraction of stars that have escaped after gas removal is still small, as most stars do not have a high enough velocity to have become spatially dissociated from the cluster (see Fig. 1 of Goodwin & Bastian [2006] and Fig. 1 of Kroupa et al. [2001]). The instantaneous mass of these young clusters thus follows: $m_{\text{cl}} \lesssim \epsilon m_c$ and, in the absence of any explicit dependence of ϵ on m_c, the CMF at such a young age mirrors the core mass function. Any meaningful comparison of our model ICMFs therefore has to be limited to populations of clusters that have either revirialized or been destroyed.

In our Monte Carlo simulations, we assume that the SFE of a core is independent of its mass. The core mass function is assumed to follow a power law of spectral index $\alpha = -2$, and we describe the probability distribution function of the SFE as a

Gaussian of mean $\bar{\epsilon}$ and standard deviation σ_ϵ, which we denote $P(\epsilon) = G(\bar{\epsilon}, \sigma_\epsilon)$.

Clearly, if the bound fraction of stars after gas expulsion, F_{bound}, depends on the core mass, then the shape of the ICMF will differ from the (power-law) core mass function, an effect whose study was pioneered by Kroupa & Boily (2002). We now take this point further by combining the detailed N-body model grid of Baumgardt & Kroupa (2007), which provides the bound fraction F_{bound} as a function of the SFE ϵ and of the ratio between the gas removal timescale τ_{GR} and the protocluster crossing time τ_{cross}.

3. THE GAS EXPULSION TIMESCALE

We model the gas expulsion from an (embedded) cluster as an outwardly expanding supershell whose radius r_s varies with time t as (Castor et al. 1975):

$$r_s(t) = \left(\frac{125}{154\pi}\frac{\dot{E}_0}{\rho_g}\right)^{1/5} t^{3/5}. \qquad (2)$$

Here $\dot{E}_0$ is the energy input rate from Type II supernovae, and ρ_g is the mass density of the residual star-forming gas in the core. We assume the mass density profiles of the core and of the newly formed stars to be alike, that is, $\rho_g = (1 - \epsilon)\rho_c$.

The energy input rate from massive stars expelling the gas is

$$\dot{E}_0 = \frac{N_{\text{GR}}E_{\text{SN}}}{\tau_{\text{GR}}}, \qquad (3)$$

where N_{GR} is the number of supernovae expelling the gas, E_{SN} is the energy of one single supernova, and τ_{GR} is the gas removal timescale. At this stage, however, we know neither N_{GR} nor τ_{GR}. Since the energy input rate from massive stars is approximately constant with time over the whole supernova phase, we thus rewrite:

$$\dot{E}_0 = \frac{N_{\text{SN}}E_{\text{SN}}}{\Delta t_{\text{SN}}}, \qquad (4)$$

where Δt_{SN} is the supernova phase duration (i.e., the time from the first to the last supernova) and N_{SN} is the total number of supernovae formed in the core. We caution that only a fraction of these contribute to gas expulsion, that is, $N_{\text{SN}} > N_{\text{GR}}$ and $\Delta t_{\text{SN}} > \tau_{\text{GR}}$.

The gas removal timescale corresponds to the instant when the supershell radius is equal to the core radius r_c, namely, $r_s(t = \tau_{\text{GR}}) = r_c$. The combination of that constraint on τ_{GR} with equations (2) and (4) gives

$$\tau_{\text{GR}} = r_c^{2/3}\left[\frac{154}{125}\frac{3}{4}\frac{\Delta t_{\text{SN}}}{N_{\text{SN}}E_{\text{SN}}}(1 - \epsilon)m_c\right]^{1/3}. \qquad (5)$$

While gas-embedded cluster masses vary by many orders of magnitude, their radii are remarkably constant, always of order 1 pc (see Kroupa 2005, Table 1). As $N_{\text{SN}} \propto m_c$, it follows from equation (5) that, for a given ϵ, the gas removal timescale τ_{GR} is independent of the core mass m_c. However, the impact of gas expulsion on a cluster is not governed by the absolute value of τ_{GR}, but by its ratio with the core crossing time τ_{cross}, i.e., F_{bound} is a function of $\tau_{\text{GR}}/\tau_{\text{cross}}$. The dynamical crossing time of the star-forming core is given by $\tau_{\text{cross}} = (15/\pi G\rho_c)^{0.5}$, which, combined with equation (5), gives

$$\frac{\tau_{\text{GR}}}{\tau_{\text{cross}}} = 1.9 \times 10^{-4}\left(\frac{\Delta t_6}{E_{51}}\frac{1-\epsilon}{\epsilon}\right)^{1/3}\left(\frac{m_c}{1\,M_\odot}\right)^{1/2}\left(\frac{r_c}{1\,\text{pc}}\right)^{-5/6}.$$
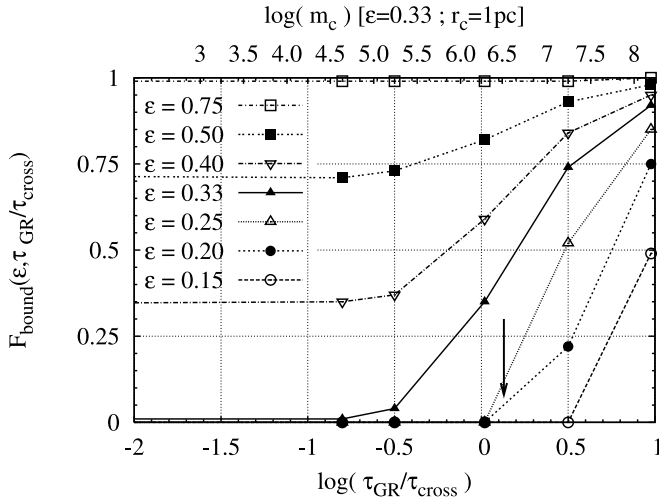
$$(6)$$

Fig. 1.—Mass fraction $F_{\rm bound}$ of stars remaining bound to the cluster at the end of the violent relaxation phase induced by gas expulsion. $F_{\rm bound}$ varies with the SFE ϵ and with the ratio between the gas removal timescale $\tau_{\rm GR}$ and the core crossing time $\tau_{\rm cross}$. The arrow indicates the bound fraction $F_{\rm bound}$ and the core mass m_c corresponding to the ICMF turnover when the mean SFE is $\bar{\epsilon} = 0.20$, and the standard deviation of the SFE probability distribution is $\sigma_\epsilon = 0.00$ (also marked by an arrow in the top panel of Fig. 2)

In this equation, the number of supernovae, $N_{\rm SN}$, from equation (5) is expressed as a function of the embedded cluster mass $m_{\rm ecl} = \epsilon m_c$, assuming a Kroupa stellar initial mass function (Kroupa 2001). We also assume that the upper stellar mass limit correlates with $m_{\rm ecl}$, as found by Weidner & Kroupa (2004), although the hypothesis of a fixed value for the mass of the most massive supernova progenitor (say, 60 $M_\odot$) hardly affects the results presented in the next section. E_{51} and Δt_6 are the energy released per supernova in units of 10^{51} ergs and the duration of the supernova phase, in Myr, respectively. In what follows, we adopt $E_{51} = 1$ and $\Delta t_6 = 30$.

Equation (6) shows that, in the absence of a mass-radius relation, the gas removal timescale, expressed in units of the core crossing time, explicitly depends on the core mass. For a given ϵ, the deeper potential well of more massive cores slows down gas expulsion when compared to low-mass cores. Massive clusters are therefore better able to adjust to the new gas-depleted potential and have a larger bound fraction $F_{\rm bound}$. Equation (6) is shown graphically in Figure 1 as a match between bottom and top x-axes for $\epsilon = 0.33$ and $r_c = 1$ pc. In the next section, we explore how the different ICMFs can be produced from the same (power-law) core mass function.

4. FROM THE CORE MASS FUNCTION TO THE INITIAL CLUSTER MASS FUNCTION

The core mass function is modeled as a power law of spectral index $\alpha = -2$ (i.e., $dN \propto m_c^{-2} dm_c$) and the distribution function for the core (local) SFE is a Gaussian, as defined in § 2. Both distributions are sampled independently, that is, the SFE is assumed to be independent of the core mass. The core radius is set to be $r_c \simeq 1$ pc, and the ratio $\tau_{\rm GR}/\tau_{\rm cross}$ is given by equation (6).

The fraction $F_{\rm bound}$ of stars remaining bound to the cluster after gas removal is inferred by linearly interpolating the grid of Baumgardt & Kroupa (2007, their Table 1), which describes how $F_{\rm bound}$ varies with ϵ and $\tau_{\rm GR}/\tau_{\rm cross}$.

According to our gas removal model, $\tau_{\rm GR}$ is the timescale over which the cluster expels the entirety of its gas. However, Baumgardt & Kroupa (2007) model gas removal as an exponential decrease with time of the cluster gas content, and their gas removal timescale
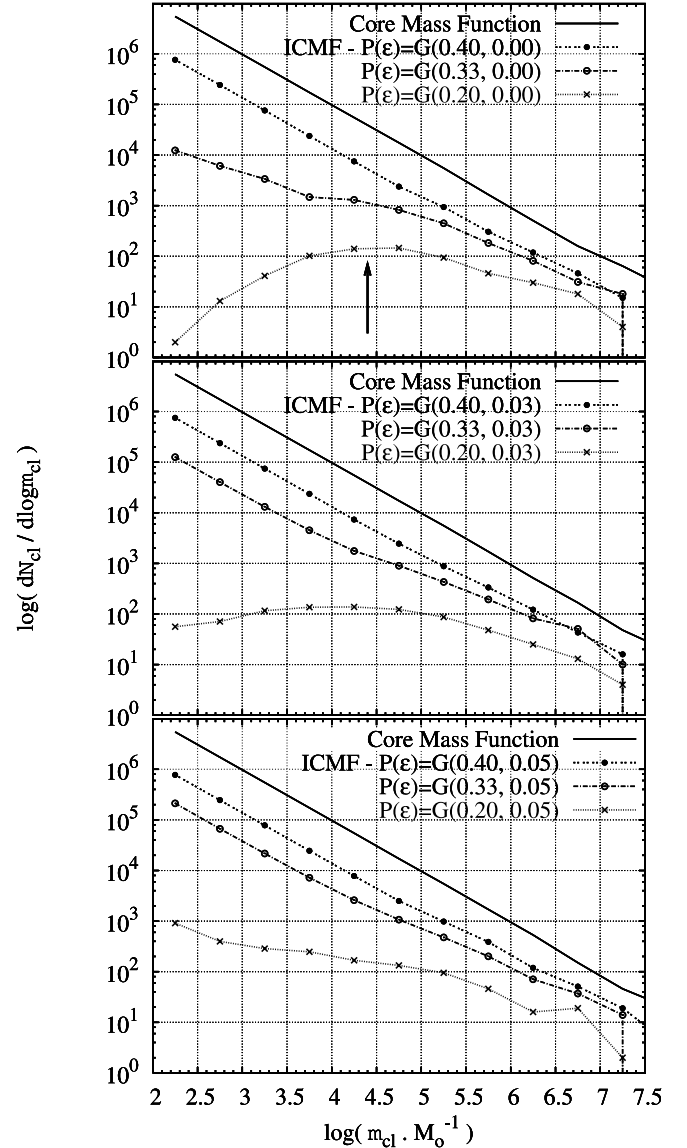

Fig. 2.—Response of the form of the ICMF produced from a -2 power-law cluster mass function to variations in the SFE Gaussian distribution $G(\bar{\epsilon}, \sigma_\epsilon)$, where $\bar{\epsilon}$ and σ_ϵ are the mean SFE and the standard deviation, respectively. Solid lines depict the original core mass function.

(τ_M in their eq. [1]) corresponds to the time when the residual gas has a fraction $e^{-1} = 0.37$ of its initial value. Prior to using their results, we multiply τ_M by a factor of 3 (i.e., $\tau_{\rm GR} = 3\tau_M$), so that $\tau_{\rm GR}$ now corresponds to a residual gas mass fraction of $e^{-3} = 0.05$; i.e., the cluster is practically devoid of gas. The corresponding grid is shown in Figure 1. In this paper, we focus on clusters evolving in a low-density environment/weak tidal field, and we thus consider the lowest half-mass radius to tidal radius ratio in the grid of Baumgardt & Kroupa (2007), i.e., $r_h/r_t = 0.01$. In stronger tidal fields the shape of the ICMF is likely to be more affected than what we find below, since low-mass clusters have smaller tidal radii and are therefore more easily disrupted by gas expulsion.

Our Monte Carlo simulations, based on equation (1) and shown in Figure 2, show the evolution of the star-forming core mass function into the ICMF. We have considered nine different cases, combining three mean star formation efficiencies ($\bar{\epsilon} = 0.20$, 0.33, 0.40) with three standard deviations ($\sigma_\epsilon = 0.00$, 0.03, 0.05). Examination of the panels of Figure 2 shows that depending on

PARMENTIER ET AL.

the assumed distribution of SFEs $G(\bar{\epsilon}, \sigma_\epsilon)$, markedly different ICMFs are produced, ranging from a power-law shape (e.g., when $\bar{\epsilon} = 0.40$, regardless of σ_ϵ) to a bell shape (e.g., when $\bar{\epsilon} = 0.20$ and $\sigma_\epsilon \lesssim 0.03$).

These different behaviors stem from the various sizes of the variations of the bound fraction F_{bound} with the core mass m_c. In order to illustrate this, let us focus on the top panel of Figure 2 for which $\sigma_\epsilon = 0$. A SFE as high as $\epsilon = 0.4$ guarantees that F_{bound} is only a weak function of the core mass m_c as $0.35 \lesssim F_{\text{bound}} \lesssim 0.95$ over the core mass range $10^3 \ M_\odot \lesssim m_c \lesssim 10^8 \ M_\odot$ (see Fig. 1). As a result, the shape of the ICMF mirrors that of the core mass function and is close to a power law of spectral index $\alpha = -2$.

In the case of a SFE of $\bar{\epsilon} = 0.33$, the same core mass range corresponds to an increase of the bound fraction with the core mass of almost 2 orders of magnitude (i.e., $0.01 \lesssim F_{\text{bound}} \lesssim 0.90$), making the ICMF significantly shallower than the core mass function. It is worth keeping in mind that the detailed form of this ICMF is uncertain, as the determination of the bound fraction F_{bound} depends on the fine details of the N-body modeling of gas expulsion when $F_{\text{bound}} \lesssim 0.1$. As for $\epsilon = 0.33$, $F_{\text{bound}} \simeq 0.01\text{--}0.04$ when $\log(\tau_{\text{GR}}/\tau_{\text{cross}}) \lesssim -0.5$ (see Fig. 1). If the bound fraction were larger over that range of gas removal timescale to crossing time ratio, the shape of the ICMF would be closer to that of the core mass function, while if F_{bound} were zero before increasing at, say, $m_{\text{core}} \simeq 10^5 - 3 \times 10^5 \ M_\odot$, this would result in a bell-shaped ICMF (see the case of $\bar{\epsilon} = 0.20$ below).

The core mass function is most affected when $\bar{\epsilon} = 0.20$. Figure 1 shows that the formation of a bound gas-free star cluster requires its parent core to be more massive than $10^6 \ M_\odot$, since the bound fraction is zero otherwise [note that the top x-axis is rightward-shifted by $\simeq 0.1$ in $\log(\tau_{\text{GR}}/\tau_{\text{cross}})$ when $\epsilon = 0.20$; see eq. (6)]. Owing to the wide variations of F_{bound} over the core mass range $(0 \lesssim F_{\text{bound}} \lesssim 0.85)$, the transformation of the core mass function into the ICMF is, in this case, heavily core mass dependent: the featureless power-law core mass function evolves into a bell-shaped ICMF. The timescale for this evolution is that required for the exposed cluster to get back into virial equilibrium following gas expulsion, that is, 50 Myr. Examination of the model grid computed by Baumgardt & Kroupa (2007) for the SFE and the gas removal timescale of relevance ($\epsilon = 0.20$ and $\tau_{\text{GR}} \gtrsim \tau_{\text{cross}}$) shows that the end of the violent relaxation phase occurs at about that age, and the cluster mass is then as defined in equation (1). As indicated by the arrows in Figure 1 and in the top panel of Figure 2, the turnover location is determined by the core mass at which the bound fraction is a few percent. For instance, a core mass of $2 \times 10^6 \ M_\odot$ with $\epsilon = 0.20$ leads to $\log(\tau_{\text{GR}}/\tau_{\text{cross}}) = 0.13$ and $F_{\text{bound}} = 0.06$. The corresponding initial cluster mass is thus $m_{\text{init}} = (0.06) \times (0.20) \times (2 \times 10^6 \ M_\odot) \simeq 2.4 \times 10^4 \ M_\odot$, roughly the mass of the ICMF turnover.

That $\epsilon = 0.20$ leads to a bell-shaped ICMF directly results from the zero bound fraction of stars for core masses less than $\simeq 10^6 \ M_\odot$. A SFE of $\epsilon = 0.25$ would result in the same effect (see Fig. 1). This is equivalent to creating a truncated power law for the *cluster-forming* cores, even though the *star-forming* core mass function is a featureless power law down to the low-mass regime. That result is reminiscent of the detailed investigation performed by Parmentier & Gilmore (2007), who found that a system of cluster parent clouds devoid of low-mass objects, such as a power-law mass function truncated at low mass, results in a bell-shaped ICMF. We emphasize that if these clusters were observed at an age of 50 Myr, their observed mass would closely match the mass predicted by our model. Actually, all clusters of the bell-shaped ICMF, irrespective of their mass, stem from gaseous progenitors more massive than $10^6 \ M_\odot$. This implies that
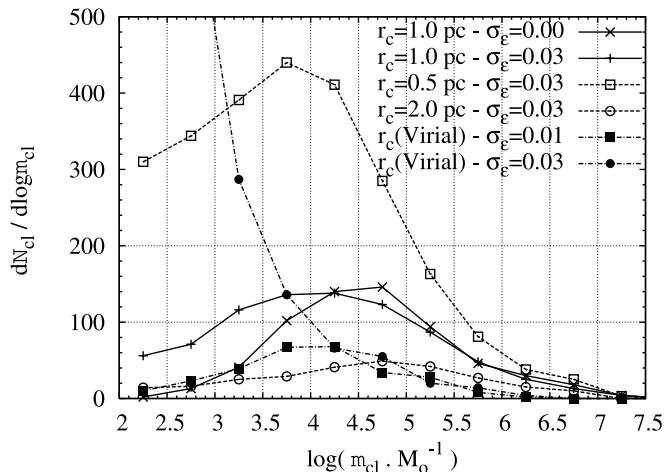

Fig. 3.—Response of the shape and position of the ICMF produced by a -2 power-law core mass function with a SFE of $\bar{\epsilon} = 0.20$ to variations in the width of the SFE distribution, and in the core radius.

unbound stars formed in the core leave the exposed cluster with velocities of order 60 km s^{-1} and do not linger as part of a halo around the bound part of the cluster. As a related consequence, note that if the very early Milky Way disk went through a violent star formation phase producing such massive clusters, then the corresponding high-velocity dispersions lead naturally to the creation of a thick disk component (Kroupa 2002).

In the middle and bottom panels of Figure 2 we show the ICMF that results from the core mass function for SFE distributions with variance $\sigma_\epsilon = 0.03$ and 0.05, respectively. The general features of the panels are the same as for zero variance; however, there are increasing differences, especially at the low-mass end of the ICMF. These differences are due to the effect of the SFE not being symmetric around the mean $\bar{\epsilon}$. For $\bar{\epsilon} = 0.2$, low-mass gas-embedded clusters with $\epsilon = 0.2$ are completely destroyed $(F_{\text{bound}} \sim 0)$, and this is the case for any cluster selected below the mean. However, a low-mass gas-embedded cluster can be drawn with $\epsilon = 0.3\text{--}0.4$, in which case it will be able to survive and retain a significant fraction of its mass. For this reason, the ICMF flattens rather than turning over in the bottom panel of Figure 2.

A key assumption underlying the above analysis is the hypothesis of a constant radius for all star-forming cores, regardless of their mass. In Figure 3, we examine the effect of the core radius on the form of the ICMF produced from a core mass function with $\epsilon = 0.20$ (i.e., a bell-shaped ICMF). We explore how the cluster mass at the turnover responds to core radius variations. A linear scaling for the y-axis is adopted as it enables us to pinpoint the turnover location more accurately. For the sake of comparison, the ICMFs obtained with $\sigma_\epsilon = 0.00$ and 0.03 and with $r_c = 1$ pc (dotted curves with crosses in top and middle panels of Fig. 2, respectively) are shown as solid lines. ICMFs depicted with open symbols correspond to constant core radius of $r_c = 0.5$ and 2 pc. A larger core radius implies smaller core densities, thereby increasing the disruptive effect of gas expulsion and lowering the number of bound gas-free star clusters. That the turnover is at higher cluster mass arises from the leftward shift of the mass scaling of the top x-axis of Figure 1 when the core radius is larger (see eq. [6]).

As stated in § 3, observations support the assumption of an almost constant core radius. This, however, is at variance with theoretical expectations that the mass-radius relation of virialized cores obeys $r_c \propto m_c^{1/2}$ (e.g., Harris & Pudritz 1994). ICMFs obtained with $r_c \text{ [pc]} = 10^{-3}(m_c/1 \ M_\odot)^{1/2}$ are shown as lines with

filled symbols in Figure 3. The normalization is such that a core of mass $10^6 \ M_\odot$ has a radius of 1 pc. Higher normalizations, corresponding to less dense cores, lead to the disruption of practically the whole original population of embedded clusters. While, for a constant core radius of $r_c = 1$ pc, the bell shape of the ICMF is preserved when σ_ϵ is increased from 0.00 to 0.03, the virial mass-radius relation leads to a power-law ICMF for $\sigma_\epsilon = 0.03$. That is, the sensitivity of the ICMF shape to the width of the distribution function for the SFE is greater than in the case of a constant core radius.

5. SUMMARY

The shape of the mass function of young star clusters remains much debated. Observational results are sorted into two distinct, often opposed, categories: power-law or bell-shaped mass functions. We have shown in this contribution that both shapes can arise from the same physical process, namely, the supernova-driven gas expulsion from newly formed star clusters on a core mass dependent timescale. Specifically, more massive cores have a higher gas removal timescale to dynamical crossing-time ratio by virtue of their deeper potential wells (assuming the near constancy of core radii over the core mass range). For a given SFE, this results in larger bound fractions F_{bound} of stars at the end of the violent relaxation that follows gas expulsion. The shape of the ICMF is chiefly governed by the probability distribution of the SFE ϵ. Bell-shaped ICMFs arise when most star-forming cores have $\epsilon \lesssim 0.25$. In that case, however, bound gas-free star clusters only form out of cores more massive than $10^6 \ M_\odot$. This implies that bell-shaped ICMFs are also associated with gas-rich environments so as to guarantee that the core mass function is sampled to such a high mass. In contrast, power-law ICMFs mirroring the core mass function arise when $\epsilon \sim 0.4$ for most star-forming cores. This implies that the shape of the ICMF also depends on the width σ_ϵ of the SFE distribution. When $\bar{\epsilon} \lesssim 0.25$, an increasing σ_ϵ enhances the contribution of cores with $\epsilon \simeq 0.40$ and turns a bell-shaped ICMF into a power law. The amplitude of that evolution is greater when core radii are assumed to follow the mass-radius relation of virialised cores than when the core radius is assumed to be constant. As illustrated by Figures 2 and 3, *that the mass function of young clusters observed in a variety of environments appears not to be universal is not surprising.*

Vesperini (1998) pointed out that a power-law ICMF of spectral index (-2) evolves to a bell-shaped mass function, the turnover of which is located at a significantly lower cluster mass than what is observed for the universal globular cluster mass function. For such models, Parmentier & Gilmore (2005) showed that a power-law ICMF with $\alpha = -2$ also leads to a radial gradient in

the peak of the evolved mass function contrary to what is observed. Baumgardt et al. (2008) demonstrated that these two issues do not arise if the ICMF is depleted in low-mass clusters compared to a power law of spectral index (-2) as a result of gas expulsion. In that case, it evolves within 13 Gyr into a cluster mass function similar to that of old globular clusters in both the inner and outer Galactic halo (see their Fig. 4). While a mean SFE of $\bar{\epsilon} \gtrsim 0.40$ preserves the shape of the core mass function, a mean SFE not exceeding $\bar{\epsilon} \simeq 0.25$ leads to a low-mass cluster depleted ICMF (see Fig. 2). The universality of the globular cluster mass function may thus stem from the existence of an upper limit of, say, 25% on the mean SFE in all protogalaxies. The origin of that constraint on the mean SFE in the protogalactic era remains to be explained, however.

In this preliminary study, the energy input rate from massive stars encompasses the contribution made by supernovae only; i.e., that of stellar winds has been neglected. Consequently, the above results apply to the sole case of metal-poor environments. As noted in § 2, we have assumed that the effect of gas expulsion depends on the actual star formation efficiency; i.e., we assume that the stars and gas (potential) are in virial equilibrium at the onset of gas expulsion. This assumption is reasonable if (the stellar component of) the cluster has had time to relax. A cluster will have been able to relax if the onset of gas expulsion occurs after a few crossing times. In a low-metallicity regime such as we are considering in this paper, gas expulsion will be driven by supernovae rather than stellar winds and so will not begin until a few Myr after the stars have formed. Such a timescale is several crossing times, and so we could expect the eSFE to closely match the SFE. We note however, that there may well be a mass-eSFE dependence in higher metallicity cluster populations that may alter our conclusions (which would be applicable to populations such as those in the Antennae merger of disk galaxies).

In a follow-up paper, we will consider the additional impact of stellar winds and the case of star clusters forming out of dense environments where strong tidal fields prevail.

REFERENCES

Anders, P., Bissantz, N., Boysen, L., de Grijs, R., & Fritze-v. Alvensleben, U. 2007, MNRAS, 377, 91
Baumgardt, H., & Kroupa, P. 2007, MNRAS, 380, 1589
Baumgardt, H., Kroupa, P., & Parmentier, G. 2008, MNRAS, 384, 1231
Bik, A., Lamers, H. J. G. L. M., Bastian, N., Panagia, N., & Romaniello, M. 2003, A&A, 397, 473
Boily, C. M., & Kroupa, P. 2003a, MNRAS, 338, 643
———. 2003b, MNRAS, 338, 673
Castor, J., McCray, R., & Weaver, R. 1975, ApJ, 200, 107
Cresci, G., Vanzi, L., & Sauvage, M. 2005, A&A, 433, 447
Elmegreen, B. G. 1983, MNRAS, 203, 1011
Elmegreen, B. G., & Clemens, C. 1985, ApJ, 294, 523
Fall, S. M., & Zhang, Q. 2001, ApJ, 561, 751
Geyer, M. P., & Burkert, A. 2001, MNRAS, 323, 988
Goodwin, S. P. 1997a, MNRAS, 284, 785
———. 1997b, MNRAS, 286, 669

Goodwin, S. P. 2008, in Young Massive Star Clusters: Initial Conditions and Environments, ed. E. Perez, R. de Grijs, & R. Gonzalez Delgado (Berlin: Springer), in press
Goodwin, S. P., & Bastian, N. 2006, MNRAS, 373, 752
Harris, W. E., & Pudritz, R. E. 1994, ApJ, 429, 177
Hills, J., G. 1980, ApJ, 235, 986
Hunter, D. A., Elmegreen, B. G., Dupuy, T. J., & Mortonson, M. 2003, AJ, 126, 1836
Johnson, K. E. 2008, in Young Massive Star Clusters: Initial Conditions and Environments, ed. E. Perez, R. de Grijs, & R. Gonzalez Delgado (Berlin: Springer), in press
Kavelaars, J. J., & Hanes, D. A. 1997, MNRAS, 285, L31
Kroupa, P. 2001, MNRAS, 322, 231
———. 2002, MNRAS, 330, 707
———. 2005, in Proc. Three-Dimensional Universe with Gaia, ed. C. Turon, K. S. O'Flaherty, & M. A. C. Perryman (ESA SP-576; Noordwijk: ESA), 629
Kroupa, P., Aarseth, S., & Hurley, J. 2001, MNRAS, 321, 699

Kroupa, P., & Boily, C. M. 2002, MNRAS, 336, 1188
Lada, C. J., Margulis, M., & Dearborn, D. 1984, ApJ, 285, 141
Mathieu, R. D. 1983, ApJ, 267, 97
Miller, B., Whitmore, B. C., Schweizer, F., & Fall, S. M. 1997, AJ, 114, 2381
Parmentier, G., & Gilmore, G. F. 2005, MNRAS, 363, 326
———. 2007, MNRAS, 377, 352
Pinto, F. 1987, PASP, 99, 1161
Spitzer, L. 1987, Dynamical Evolution of Globular Clusters (Princeton: Princeton Univ. Press)

Verschueren, W. 1990, A&A, 234, 156
Verschueren, W., & David, M. 1989, A&A, 219, 105
Vesperini, E. 1998, MNRAS, 299, 1019
Weidner, C., & Kroupa, P. 2004, MNRAS, 348, 187
Whitmore, B. C., Zhang, Q., Leitherer, C., Fall, S. M., Schweizer, F., & Miller, B. W. 1999, AJ, 118, 1551